Applied Thermal Engineering 73 (2014) 586–595

Contents lists available at ScienceDirect

Applied Thermal Engineering

journal homepage: www.elsevier.com/locate/apthermeng

Electricity generation from an exhaust heat recovery system utilising thermoelectric cells and heat pipes

B. Orr*, B. Singh, L. Tan, A. Akbarzadeh

Energy Conservation and Renewable Energy (Energy CARE) Group, School of Aerospace, Mechanical and Manufacturing Engineering (SAMME), RMIT University, Bundoora East Campus, 3083 Bundoora, Australia

HIGHLIGHTS

- Car exhaust heat recovery design.
- Unique design that utilises heat pipes and thermoelectric cells.
- System is solid state and passive.
- The electrical power produced was 6.03 W.
- The resultant efficiency of the system was 1.43%.

ARTICLE INFO

Article history:
Received 7 March 2014
Accepted 20 July 2014
Available online 26 July 2014

Keywords:
Exhaust heat recovery
Heat pipes
Thermoelectric cells

ABSTRACT

The internal combustion engine used in majority of cars at the present time do not use their fuel input very efficiently. A majority of this energy is dissipated as heat in the exhaust. The related problems of global warming and dwindling fossil fuel supplies has led to improving the efficiency of the internal combustion engine being a priority. One method to improve the efficiency is to develop methods to utilise heat in car exhausts that is usually wasted. Two promising technologies that were found to be useful for this purpose were thermoelectric cells (TECs) and heat pipes. Therefore this project involved making a bench type, proof of concept model of power production by thermoelectric cells using heat pipes and hot engine exhaust gases. 8 cells were used and managed to produce 6.03 W when charging the battery. The system operated with a heat to electricity conversion efficiency of 1.43%. The discrepancy between the actual efficiency and the predicted efficiency of 2.31% is most likely due to the cells not operating at their optimum voltage. The predicted efficiency is approximately 1/9 of the Carnot efficiency and the actual efficiency is approximately 1/15 of the Carnot efficiency.

1. Introduction

The automobile industry has been identified as one of the target industries for the reduction of greenhouse gas (GHG) emissions therefore much research has been undertaken in this area. Despite this intensive research, there have been no clear viable alternatives to the fossil fuelled internal combustion engines (ICE). As progress has been slow in that respect, research must be undertaken to improve the current ICEs efficiency to preserve current fossil fuel supplies until a viable alternate presents itself. Current ICEs are approximately 25% efficient (Fig. 1) under typical driving conditions (i.e.: European driving cycle). Therefore there is lots of room for improvement. Most of the losses for ICEs are heat losses. Therefore this is one area to be targeted. Most of the heat losses can't be prevented therefore methods must be developed to utilise this heat. A lot of this heat is of a lower grade and difficult to utilise. The two areas where the heat is easier to utilise are the exhaust gases and the engine coolant. Engine coolant can only reach a maximum of approximately 90 °C [1]. This is a lower grade of heat than exhaust gases that can reach maximum temperatures of over 400 °C. Approximately 40% of the energy used is wasted in the exhaust gases as shown in Fig. 1. Therefore it is most viable to utilise the exhaust gas heat. This paper identifies TECs and heat pipes for use in an exhaust heat recovery system.

TECs make use of what is known as the Seebeck effect. When one side of the cell is heated and the other side cooled, a voltage is generated. The voltage generation means there are applications for

* Corresponding author.
E-mail addresses: bradley.g.orr@gmail.com, s3236808@student.rmit.edu.au (B. Orr).

http://dx.doi.org/10.1016/j.applthermaleng.2014.07.056
1359-4311/

Nomenclature

I	electric current [A]
I_{SC}	cell short circuit electric current [A]
P	electrical power of the system [W]
P_{Carnot}	potential power of system at Carnot efficiency [W]
$P_{predicted}$	power of the system at predicted efficiency [W]
$P_{TEC\ Carnot}$	potential power of individual TEC at Carnot efficiency [W]
$P_{TEC\ predicted}$	power of individual TEC at predicted efficiency [W]
$\dot{Q}$	rate of heat transfer [W]
$\dot{Q}_{in}$	Rate of heat input [W]
R	thermal resistance [°C/W]
T	temperature [°K]
ΔT	temperature difference [°C]
T_c	heat engine minimum operating temperature [°K]
T_h	heat engine maximum operating temperature [°K]
V	voltage [V]
V_{OC}	cell open circuit voltage [V]
ZT	TEC figure of merit

Greek symbols

η	heat to electricity conversion efficiency of the system [%]
η_{Carnot}	Carnot efficiency of the system [%]
$\eta_{predicted}$	predicted efficiency of the system [%]
$\eta_{TEC\ Carnot}$	Carnot efficiency of individual TEC [%]
$\eta_{TEC\ predicted}$	predicted efficiency of individual TEC [%]

these cells to generate electricity where temperature differences are present. This makes them heat engines much like ICEs. The advantages they have over mechanical heat engines are that they are silent, very small, completely scalable and durable. Their key advantage is that they have no moving parts and no chemical reactions therefore there is little maintenance required due to wear and corrosion. Their efficiency is typically 5% [3] compared to about 25% for ICEs but they can generate power from any temperature difference unlike ICEs. As with all heat engines, their efficiency is limited by the Carnot efficiency so the higher the temperature difference, the more efficient they will be. Heat engines have rejected heat which is why one side needs to be cooled.

A heat pipe is a metallic pipe that is sealed at both ends and is partially filled with a fluid at vacuum pressure. Heat pipes are very good heat conductors therefore they are used to transfer heat relatively long distances quickly and efficiently. Their thermal conductivity can be magnitudes higher than copper. A typical use of a heat pipe would be in a laptop computer. In laptops, they are used to transfer heat from the CPU somewhere in the middle of the motherboard to a heat sink on the edge of the motherboard exposed to ambient air. A heat pipe is a completely passive heat transfer device. No fans or moving parts are needed.

2. Current state of the art

Large multinational car companies like BMW [4], Ford [5] and Honda [6] have demonstrated their interest in exhaust heat recovery, developing systems that make use of TECs. Their method was to connect the circular exhaust to an expansion chamber using a flange. One side of the cells was placed on the faces of the expansion chamber and the other side of the cells was cooled by a liquid coolant. The coolant could be from the main car radiator or an independent radiator. This technology has not yet been installed in present production cars and is still in the concept stages. There are many similar designs with the differences being the shape of the expansion chamber (i.e.: hexagonal) and the method of cooling (i.e.: air cooled).

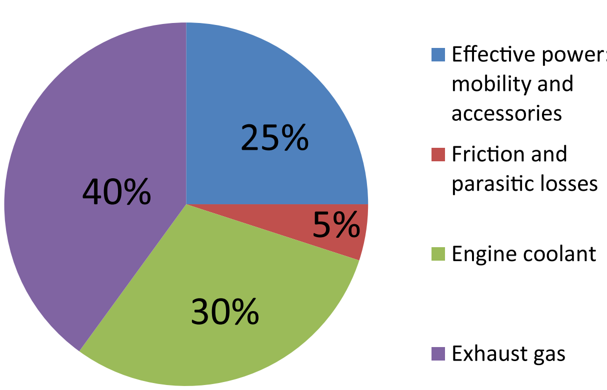

Fig. 1. Energy distribution of a typical ICE [2].

A waste heat recovery system has been developed to replace a traditional car radiator [2,7]. The aim was to replace the radiator without introducing an extra moving component. Only existing moving components like the water pump and fan were used. The use of heat pipes and TEGs allowed for heat transfer and power production without introducing extra moving parts. This system makes use of the waste heat in the coolant rather than the exhaust gases. The system consisted of 72 TEGs of 40 mm by 40 mm size. 128 small diameter heat pipes were used. During idle conditions the hot side was approximately 90 °C and the cold side was approximately 70 °C. During these conditions 28 W were produced. When run in the driving mode of 80 km/h, the hot side was approximately 90 °C and the cold side was approximately 45 °C. During these conditions 75 W were produced.

There are two examples of exhaust heat recovery using both thermoelectric cells and heat pipes. For the first example [8], the exhaust gases flow through an exhaust pipe with heat pipes protruding through. The heat pipes absorb some of the heat and spread it through the aluminium block they are inserted into. The hot side of the thermoelectric cells are placed on the surface of the aluminium block. The rejected heat from the cells is removed by a water cooled heat sink placed on the other side of the cells. This system generated a maximum of 350 W using 112 40 mm × 40 mm thermoelectric cells.

The second example [9–11] works in a similar way by using the heat pipe to extract the heat from the exhaust gases to the hot side of the thermoelectric cells and using a water heat sink to cool the other side of the cells. In this case a variable conductance heat pipe (VCHP) is used instead of a standard heat pipe. A VCHP operates in the same way as a standard heat pipe but can maintain a steady operating temperature. A VCHP contains non condensable gases inside. With increasing heat load, these gases are pushed up the heat pipe and into the expansion tank. This increases the length of the condensing section. Therefore with an increasing heat load, the operating temperature does not change because of the increasing condenser length removing more heat. Keeping a steady heat pipe operating temperature despite varying heat loads is useful when using thermoelectric cells because the cells can fail when operating over their rated maximum temperature.

A prototype exhaust heat recovery system was implemented into a bus for the purpose of interior heating [12]. The system uses heat pipes to extract the heat from the exhaust gases and transfers

this heat to the fresh ambient air. This air is ducted into the bus cabin. Typical automotive heaters use waste heat from the engine coolant but this might not be sufficient for the large bus cabin. This system prevents the need for extra supplementary heaters to be installed consequently saving fuel. The system was not designed to produce electricity.

The most popular form of thermoelectric material is Bismuth Telluride. TECs using this material are typically used as heat pumps because of their favourable properties at close to room temperature. Their use as generators is limited because their maximum hot side operating temperature is relatively low. As they are widely used and mass produced, their cost is low compared to other thermoelectric materials. Other materials and techniques have been used to improve the power generation and efficiency of TECs. Lead Telluride has been used as a material in TECs designed for power generation. These TECs are able to handle the higher temperatures. This means a larger temperature difference can be present and potentially more power and higher efficiency can be achieved. Some TECs have been manufactured with segmented material. A material with a high ZT at higher temperatures is used on the hot side (i.e.: Lead Telluride) and a material with a high ZT at lower temperatures is used on the cold side (i.e.: Bismuth Telluride). More power would be produced compared to a TEC made of just the high temperature rated material. Other materials such as Skutterudites and other manufacturing techniques such as quantum well structures have been investigated to improve TEC power generation efficiency [13].

Heat pipes have been used in conjunction with TECs for the purpose of power generation in solar power applications [14]. One design uses heat pipes and TECs in a concentrated solar thermal power generation system. The concentrated sunlight heats up the hot side of the cell and the finned heat pipes cool the cold side of the cell. The temperature difference over the TEC allows for electricity to be generated. Another design uses heat pipes and TECs in a solar pond. A solar pond has a temperature gradient from the top surface to the bottom surface. The hot side of the TECs are heated by the hot water at the bottom surface. The cold side is cooled using heat pipes and the cooler water at the top surface.

These previous works above give a broad overview of what has been undertaken in this area of research. There are some potential gaps in the literature though. For the application of exhaust heat recovery, there is very little evidence at the time of printing of anything other than engine coolant being used to cool the TECs. The use of engine coolant requires the use of mechanical pumps and active monitoring systems. A potential area to be addressed is to design a system which is both completely passive and solid state.

3. Proposed system of power production by thermoelectric cells using hot engine exhaust gases

Both thermoelectric cells and heat pipes have very promising attributes for their use in exhaust heat recovery systems. The fact that TECs have no moving parts and their ability to generate electricity from lower temperature heat sources are what make them attractive for this situation. Heat pipes have the same advantage of not introducing moving parts. Their high thermal conductivity allows for heat to be transferred over significant distances with very little temperature drop. Heat sinks without heat pipes have long fins. This causes its fin efficiency to be low due to the large distance between the fin tip and the base surface. Heat sinks with heat pipes have relatively high fin efficiency due to the small distance between the fin tips to the heat pipe. The thermal resistance of the heat pipe to the base surface is low. This means that typically a heat sink with integrated heat pipes will have a lower thermal resistance than a heat sink without integrated heat pipes. Their lower thermal resistance allows the hot side of the TECs to be closer to the exhaust gas temperature. Considering these promising attributes, it was decided that this project will utilise both technologies for the purpose of exhaust heat recovery.

This project is intended to be a proof of concept. It will be a bench type model but real life applications of this project would be for exhaust heat recovery in typical passenger cars. The electrical power demands of modern passenger cars are increasing therefore the demand on the alternator is increasing. The alternator is driven by the engine therefore the higher the alternator load, the higher the engine fuel consumption. Electricity generation from an implemented exhaust heat recovery system could completely replace the alternator or reduce its load therefore saving fuel. For this project, the electricity generated will be used to charge a 12 V battery as it would in a typical passenger car.

There are a couple of potential problems with implementing a system like this into a car. A heat exchanger implemented into an exhaust system would introduce back pressure. This means that the pumping losses of the engine would increase due to the extra power required to expel the exhaust gases. The extra weight of the system would also negatively affect the fuel economy but this is slightly offset by reducing the size of the alternator or completely removing it altogether. If the system is to be viable, it must have a net positive impact on the fuel economy of the car.

A simplified diagram of the testing rig design can be seen in Fig. 2. One novelty of this design compared to others is that heat pipes are also used to cool the thermoelectric cells whereas in all other designs engine coolant is used. Engine coolant is maintained at 90 °C and atmospheric air is approximately 20 °C. This means there is a potential to have a higher temperature difference over the cells using air cooled heat pipes which is why this is the design direction that has been taken. The use of cooling fluid requires the use of a mechanical pump which is undesirable. As heat pipes are used to both cool and heat the TECs, the second novelty of this design is that the system is a completely passive, solid state design.

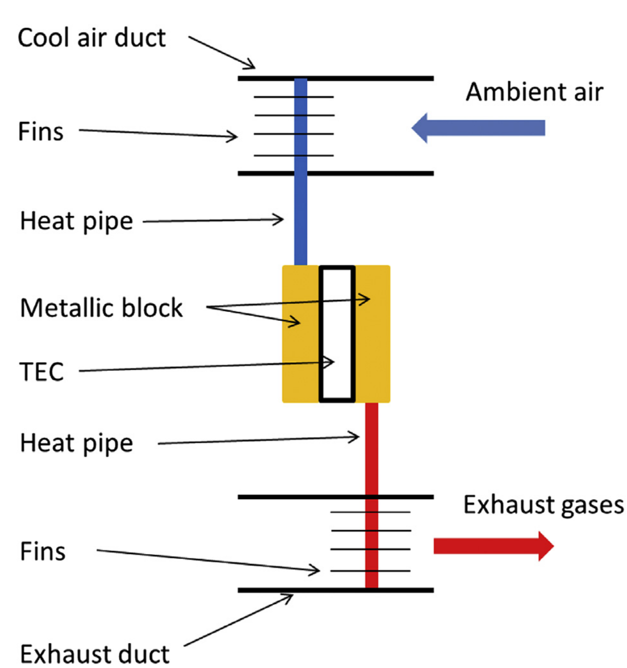

Fig. 2. The proposed concept for the exhaust heat recovery system.

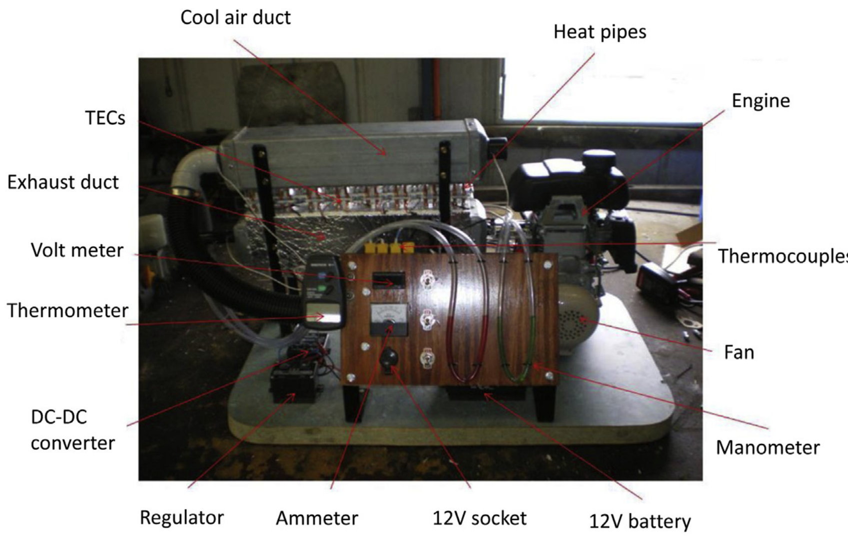

Fig. 3. Testing rig components.

4. Testing rig

The heat pipes used in the testing rig were not designed to be under any compressive load. Therefore 4 steel braces were used to take the load off the heat pipes and to secure the system to the base (Fig. 3). Using the braces not only prevents the heat pipes from buckling, it also makes them less susceptible to the cyclic loads due to the vibration.

The heat sink that was selected for the testing rig was originally designed as a CPU (Central processing unit) cooler. It was not possible to have a custom made heat sink due to budget and time constraints. There are 2 6 mm copper/water heat pipes used in each heat sink (Figs. 4 and 5). Although CPU coolers do not experience temperatures as high as in this case, heat pipes with water as a working fluid can operate up to approximately 200 °C [15]. The exhaust gas temperatures do exceed this temperature but due to the very small exhaust gas mass flow rate, the thermal resistance of the fins is relatively high. This means the heat pipe operating temperature would be closer to the cell surface temperature than the exhaust temperature. Despite this fact it is likely that some of the heat pipes were outside of their operational temperature range. The heat pipes heating cell number 1 were discoloured after use indicating that they were likely to be operating over their temperature limit. The measured rate of heat transfer through some modules would be very close to the maximum rate of heat transfer of the 2 heat pipes combined.

5. Results and discussion

5.1. Improving power output

Before any official testing was undertaken, preliminary tests were completed to determine the effects of adding a DC–DC converter and insulation to the testing rig. The DC–DC converter was connected in-between the cells and the regulator. It doubles the input voltage and halves the input current. Using this device allows the cells to operate at half their normal operating voltage and still charge a 12 V battery. Consequently the cells operate closer to their optimum voltage and more power is produced. The optimum voltage of a TEC is half the open circuit voltage. Another method to increase the amount of power produced by the cells was to reduce the heat losses in the exhaust pipe and exhaust duct using

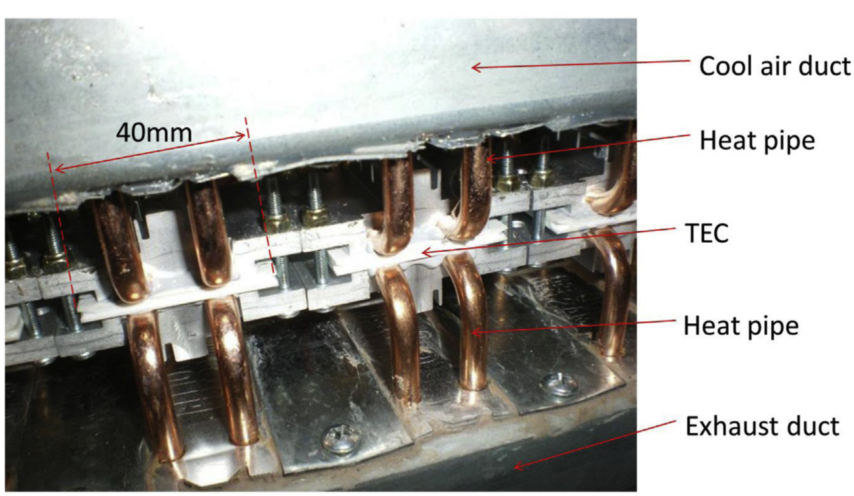

Fig. 4. Close up of the ducts, heat pipes and cells.

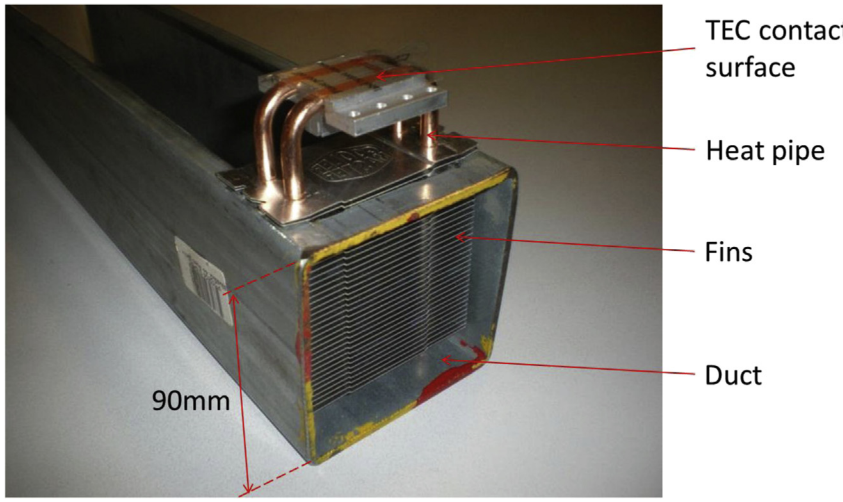

Fig. 5. Fins inside the ducts attached to the heat pipes.

insulation. The trapping of heat by the insulation should increase the temperature difference over the cells. Therefore the cells have a higher open circuit voltage and consequently can produce more power. The power increases can be seen in Table 1.

5.2. Cell operating temperatures and temperature profile

Fig. 6 is a graphical interpretation of the cell face temperatures and temperature differences. Table 2 is the tabular version of this data. Cell 1 is the cell closest to the engine and cell 8 is the outmost cell. There seems to be a significant reduction in temperature difference between the 3rd and 5th cell. This may be because the exhaust mass flow rate is magnitudes smaller than the cooling duct mass flow rate therefore the temperatures converge quickly. If a smaller length duct was used or a bigger engine, the temperature difference distribution may look more like a typical counter flow heat exchanger. Another possible reason for the drop in temperature difference could be due to the heat pipes. The water heat pipes used have a minimum operating temperature of approximately 30 °C [15]. Below this temperature the heat pipes don't work. Above this temperature the heat pipes just start to operate. The heat pipes

Table 1
Changes in power due to the addition of a DC–DC converter and insulation.

	Voltage (V)	Current (A)	Power (W)	Power change
Baseline	14.4	0.26	3.74	–
With DC–DC converter	14.4	0.34	4.90	+30.77%
With DC–DC converter + insulation	14.4	0.40	5.76	+53.85%

Table 2
Cell surface operating temperatures.

Cell number	T_{hot} (°C)	T_{cold} (°C)	Delta T (°C)
1	198	78	120
2	195	79	116
3	172	68	104
4	118	52	66
5	57	39	18
6	45	35	10
7	40	32	8
8	38	31	7

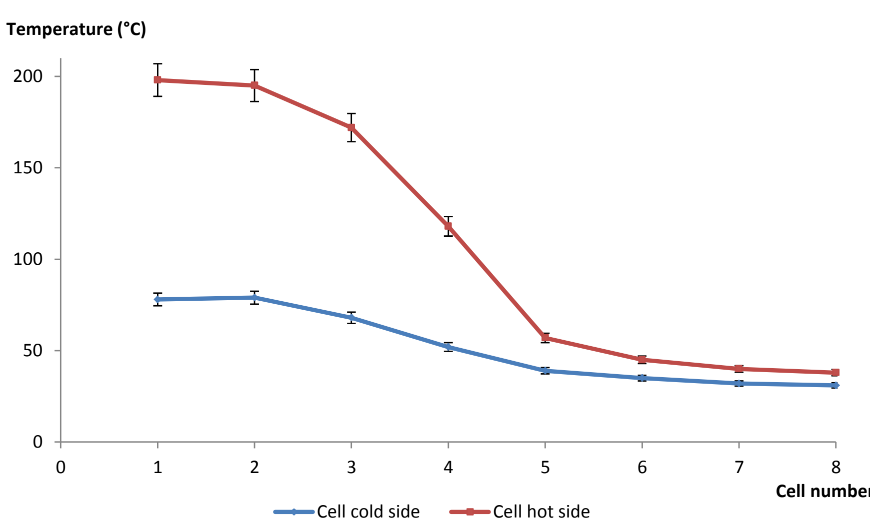

Fig. 6. Cell temperature difference profile along the duct.

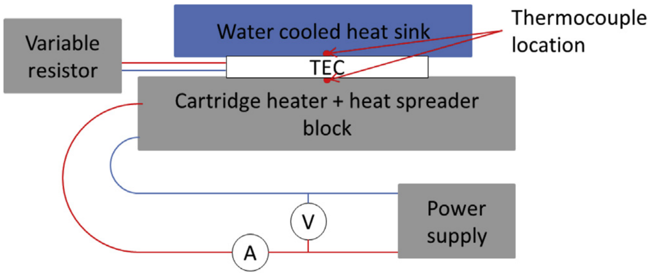

Fig. 7. Schematic of thermoelectric cell testing rig.

Table 3
Calculation of cell thermal resistance and ZT.

Heat input (W)	T_{hot} (°C)	T_{cold} (°C)	Delta T (°C)	P_{max} (W)	V_{oc} (V)	R_{th} (°C/W)	ZT
5	24.84	19.68	5.16	0.01	0.24	1.03	0.48
10	32.18	20.85	11.32	0.04	0.51	1.13	0.50
20	44.85	23.16	21.70	0.15	0.99	1.08	0.52
40	69.69	27.58	42.11	0.48	1.92	1.05	0.45
60	95.73	32.26	63.47	1.08	2.95	1.06	0.47
80	123.23	36.95	86.28	1.84	3.97	1.08	0.46
100	148.04	41.16	106.88	2.70	4.95	1.07	0.46
120	170.14	45.37	124.77	3.54	5.70	1.04	0.44
					Ave	1.07	0.47

heating and cooling cells 5–8 would be very close to the minimum operating temperature. Effectively, these heat pipes would have a high thermal resistance compared to the others resulting in a smaller temperature difference over the cells. The small temperature difference over the last 4 cells means they contribute little to the generated power. There is some error involved with the measurements. The thermocouple thermometer used has a stated accuracy of ±1 °C. This is quite a large percentage of error when the temperature difference is a single digit number. The cells were measured for temperature at one point as it was assumed that the entire surface was isothermal. This would not be the case in reality. Despite these errors, the results are relatively accurate and trustworthy. When the test was repeated, the maximum difference between the two same data points was 4.5% hence the error bars in Fig. 6 are 4.5%.

5.3. Calculation of system efficiency

A method was required to determine the heat input to the system which did not need measurements of mass flow rates and flow velocities. As all the heat input to the system must pass through the thermoelectric cells, if the temperature difference across the cells is known and the thermal resistance of the cells is known then the heat flow through the cells can be determined. Therefore a test was conducted to determine the thermal resistance of the cells in use. A testing rig similar to the one in Figs. 7 and 8 was used for this purpose. This testing rig consists of a cartridge heater, thermoelectric cell (Fig. 9), 2 thermocouples, water cooled heat sink, amp meter and a volt meter. Equation (1) was used for the calculation of the thermal resistance. The power supplied to the cartridge heater was measured using the volt and amp meters. It was assumed that the cartridge heater was 100% efficient and all heat produced by the cartridge heater travels through the cell. The thermocouples were used to measure the cell hot and cold side surface temperatures. This information was used to determine the thermal resistance of the cells at different levels of heat input and then the average thermal resistance was measured (Table 3). Using equation (2), a similar method was used to determine the average ZT of the cell. This would be the thermal resistance value and ZT value used for further calculations.

$$R = \frac{\Delta T}{\dot{Q}} \tag{1}$$

$$P_{\text{TEC predicted}} = \left(1 - \frac{T_c}{T_h}\right)\dot{Q}_{in}\frac{\left(\sqrt{ZT+1}\right) - 1}{\left(\sqrt{ZT+1}\right) + \frac{T_c}{T_h}} \tag{2}$$

$$\therefore R = 1.07\frac{^{\circ}C}{W} \tag{3}$$

$$\therefore ZT = 0.47 \tag{4}$$

Now that the thermal resistance of the cells had been determined and knowing the cell surface temperatures from Table 2, the heat flow rate through each individual cell can be determined using equation (5). This is shown in Fig. 10. The heat flow rate into the system is the summation of the heat flow rate through each individual cell (Equation (6)). The power generated by the cells had

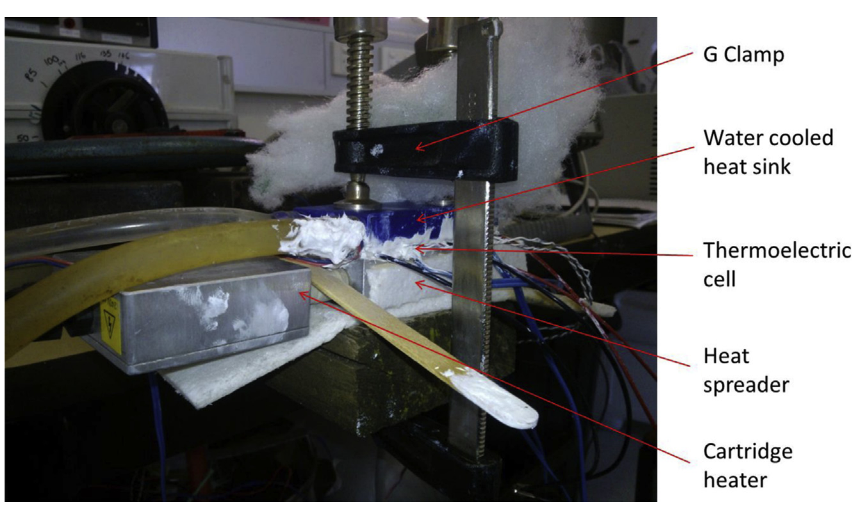

Fig. 8. Thermoelectric cell testing rig.

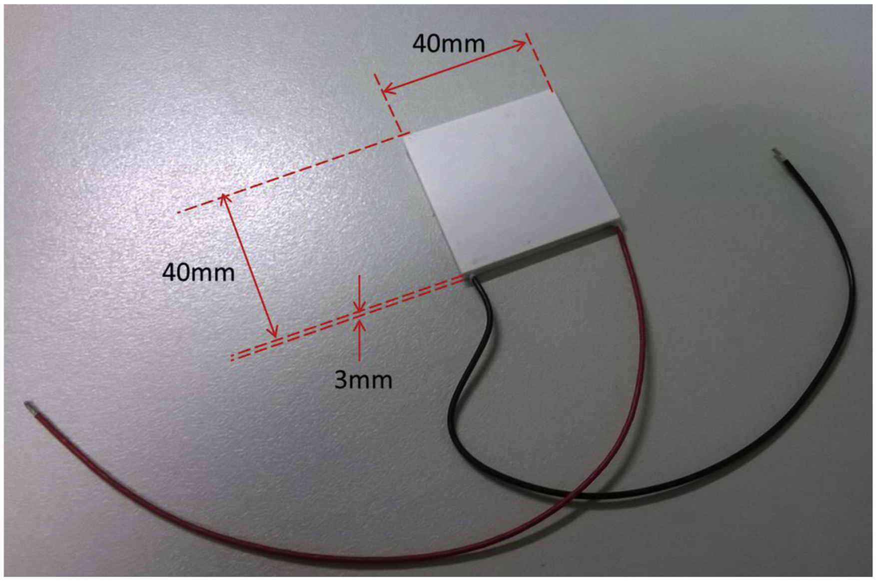

Fig. 9. The TEC tested.

been measured therefore the system efficiency could be calculated as seen in equation (7). This system efficiency is comparable with similar systems that make use of TECs [3,5].

$$\dot{Q} = \frac{\Delta T}{R} \tag{5}$$

$$\dot{Q}_{\text{in}} = \sum \dot{Q}_{\text{Cells}} \qquad \dot{Q}_{\text{in}} = 420.34W \tag{6}$$

$$\eta = \frac{P}{\dot{Q}_{\text{in}}} \qquad \eta = 1.43\% \tag{7}$$

5.4. Calculation of predicted system efficiency

The Carnot efficiency is the maximum possible efficiency of a heat engine when operating between the two different temperatures T_c and T_h. When considering the entire exhaust heat recovery system, T_h is the exhaust duct inlet temperature and T_c is the cool air duct inlet temperature. During the testing the exhaust duct inlet temperature was 600 °C and the cool air duct temperature was 20 °C. Unfortunately, the top and bottom surface temperatures over all 8 cells are not the exhaust duct inlet temperature and cool air duct inlet temperature respectively. This is due to the thermal resistance of the heat exchanger. The thermal resistance of the gas to the fins, the fin efficiency, the heat pipes, the aluminium block and thermal paste etc. would result in a temperature drop from the gas to the cell surface. This means that the Carnot efficiency considering the temperature difference of the cells will be lower than the overall Carnot efficiency. Each individual cell has a different temperature difference therefore will have a different Carnot efficiency. Equation (8) can determine the maximum

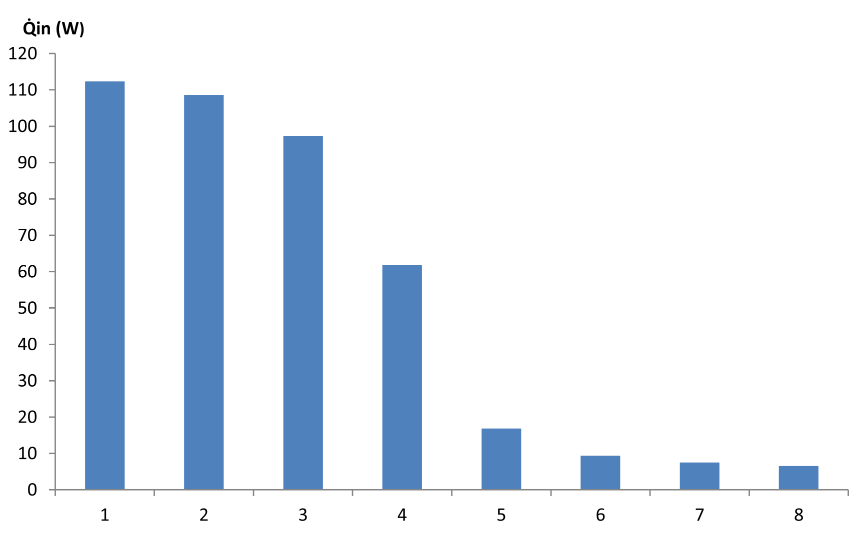

Fig. 10. Rate of heat input for each individual cell.

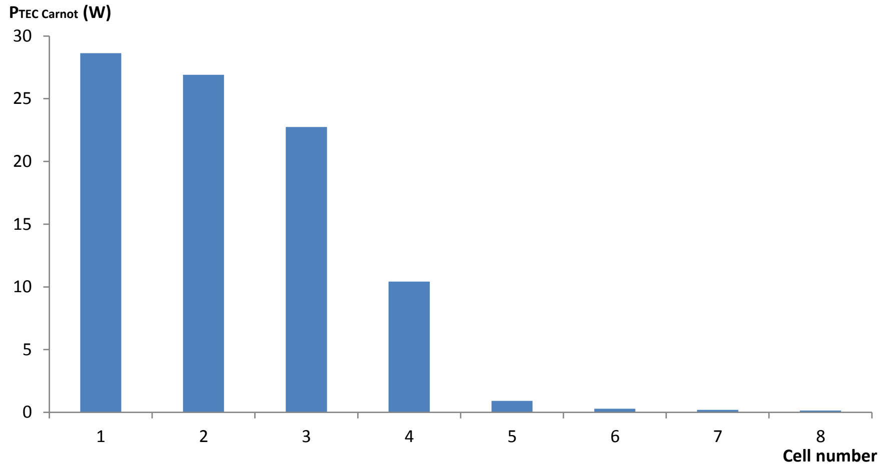

Fig. 11. The potential power from each individual cell.

potential power each cell can produce knowing the cell surface temperatures from Table 2 and the heat flow rates from Fig. 10. Fig. 11 shows the calculated maximum potential power for each individual cell. The sum of each cell's maximum potential power (Equation (9)) is the maximum potential power of the system when considering cell surface temperatures for the Carnot efficiency. The actual Carnot efficiency of the system when considering cell surface temperatures (Equation (10)) can be found by dividing the power found in equation (9) by the known heat input found previously in equation (6). It can be seen that the actual efficiency is approximately 1/15 of the Carnot efficiency.

$$P_{\text{TEC Carnot}} = \left(1 - \frac{T_c}{T_h}\right)\dot{Q}_{\text{in}} \tag{8}$$

$$\begin{aligned} P_{\text{Carnot}} &= \sum P_{\text{TEC Carnot}} \\ P_{\text{Carnot}} &= 90.27W \end{aligned} \tag{9}$$

$$\begin{aligned} \eta_{\text{Carnot}} &= 21.48\% \\ \eta_{\text{Carnot}} &= \frac{P_{\text{Carnot}}}{\dot{Q}_{\text{in}}} \end{aligned} \tag{10}$$

Equation (11) below can be used to predict the power produced by an individual cell. This is a modified version of an equation used by Stobart et al. [13]. If the surface temperatures of the cell are known, the rate of heat transfer through the cell is known and the ZT of the cell is known, it is possible to predict the power the cell will produce. This is shown in Fig. 12. An average value of ZT was determined as seen in Table 3. The sum of the predicted power of each individual cell is the predicted power of the system (Equation (12)). The predicted efficiency can be found by dividing the predicted power by the known rate of heat transfer of the system (Equation (13)). It can be seen that this method over predicts that actual power produced. There a number of possible reasons for this. Firstly, this method assumes that each individual cell is operating at its maximum power. This would not be the case. As all the cells are connected in series, the same current flows through each cell. Due

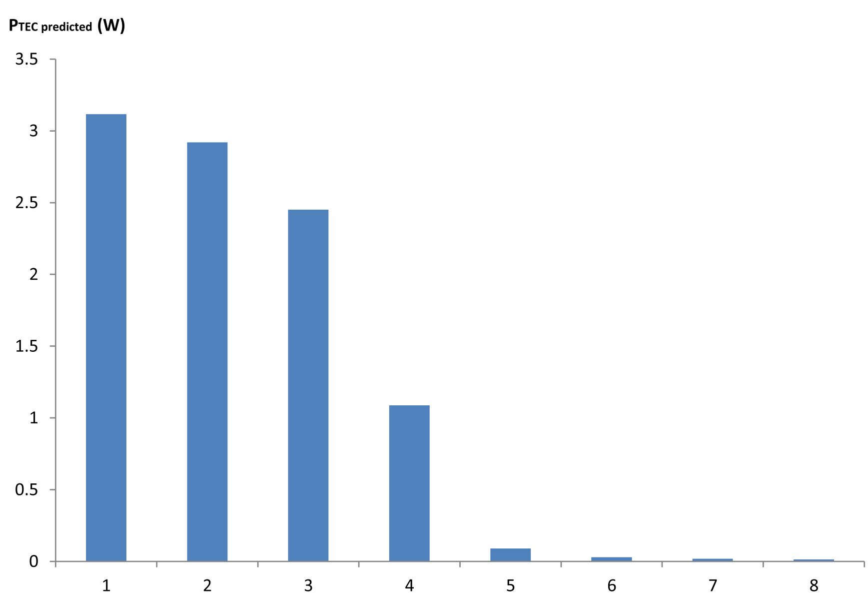

Fig. 12. The predicted power from each individual cell.

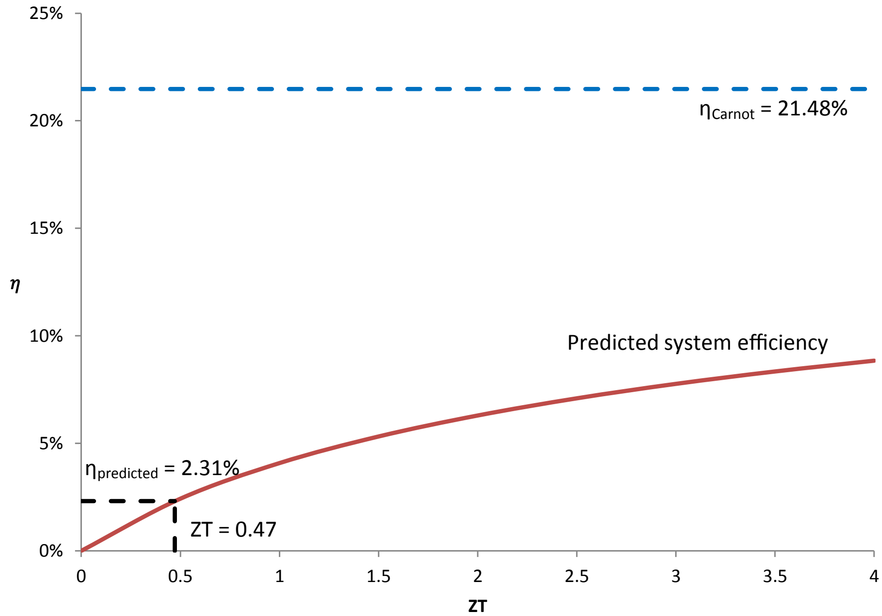

Fig. 13. System efficiency vs. ZT of a TEC.

to the different operating conditions of each cell, they would have different optimum currents. Secondly, the ZT of bismuth telluride cells is not constant with temperature and not constant between different manufacturers [16]. This could mean that the assumed value of ZT is too high. Despite the over predictions, this method calculated system efficiencies which are in line with other experimental results of similar systems.

$$P_{\text{TEC predicted}} = \left(1 - \frac{T_c}{T_h}\right)\dot{Q}_{\text{in}}\frac{\left(\sqrt{ZT+1}\right) - 1}{\left(\sqrt{ZT+1}\right) + \frac{T_c}{T_h}} \tag{11}$$

$$\begin{aligned} P_{\text{predicted}} &= \sum P_{\text{TEC predicted}} \\ P_{\text{predicted}} &= 9.73W \end{aligned} \tag{12}$$

$$\begin{aligned} \eta_{\text{predicted}} &= \frac{P_{\text{predicted}}}{\dot{Q}_{\text{in}}} \\ \eta_{\text{predicted}} &= 2.31\% \end{aligned} \tag{13}$$

Fig. 13 below gives a clear indication of the potential for improvement in the system. It can be seen that the predicted efficiency of the system is well off the Carnot efficiency of the system. The predicted efficiency is approximately 1/9 of the Carnot efficiency. Assuming the heat exchanger design remains as is, if the cells currently in use are replaced with cells of a higher ZT, the system efficiency would increase. At the present time, maximum reported ZT values are approximately 1.2 [17]. Even if cells with a ZT of 1.2 are used, the predicted efficiency would only increase to approximately 5%. The predicted efficiency curve asymptotes at the Carnot efficiency as ZT approaches infinity.

Table 4
Comparison of power produced when connected to the battery and variable resistor.

	Voltage (V)	Current (A)	Power (W)	Power change
Max power (Variable resistor)	9.70	0.69	6.71	–
Max power (Charging battery)	13.70	0.44	6.03	−10.22%

5.5. *Determination of maximum potential power*

The maximum power that was produced by the cells when charging the battery was found to be 6.03 W (Table 4). Using a variable electric load, the maximum potential power the cells can generate under the same conditions was found. The cells were disconnected from the battery and connected to the device. Measured data from this device is shown in Fig. 14. The data was as expected with a linear relationship between voltage and current. It was found that the maximum potential power the cells can generate was 6.71 W. The small difference between the max potential and actual power means that the cells are operating close to their optimum voltage. The voltages and currents displayed in Table 4 for the maximum power generated when charging the

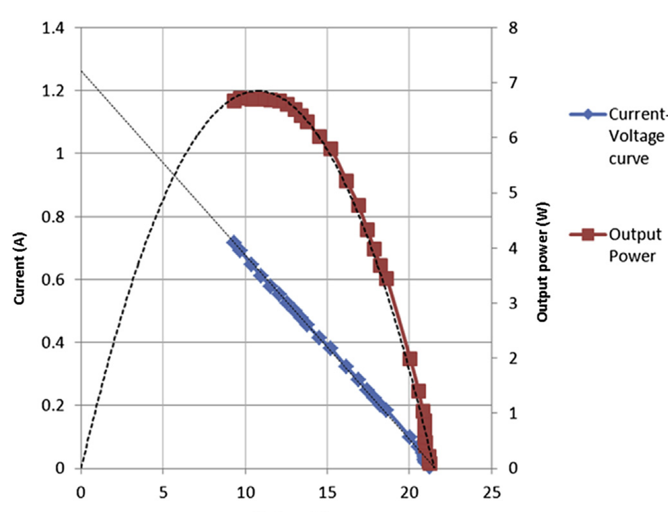

Fig. 14. Cell output power and *I*–*V* curve.

battery is measured after the DC–DC converter. Previous preliminary tests found that the cells actually operate at about 8 V when charging the battery. Table 4 indicates that the optimum voltage was 9.7 V so as the cells operate just below the optimum voltage, they produce slightly less power. Although all the cells as a whole may be operating close to the optimum voltage, individual cells may not be operating at their optimum voltage. All the cells are producing different voltages and are most likely not operating at half their open circuit voltage. If all the cells produced the same voltage, then they would be operating at their individual optimum voltage. It is possible that the power losses from the current flowing through the last 4 cells are greater than the power generated from them meaning the last 4 cells could be a hindrance.

6. Conclusion

Investigations have found that an appropriate way of improving the overall efficiency of the fuel use in a car is to recover some of the wasted heat in its exhaust. Two technologies identified to be of use for exhaust heat recovery are thermoelectric cells and heat pipes. A proof of concept, bench type model has been completed and working as expected. 8 cells were used and managed to produce 6.03 W when charging the battery. This was not far off the maximum power produced using the variable resistor device therefore they are operating close to their optimum voltage. The heat to electricity conversion efficiency of the system was 1.43%. The higher predicted efficiency of 2.31% is due to each individual cell not operating at its optimum voltage/current. This predicted efficiency is approximately 1/9 of the calculated Carnot efficiency. The actual efficiency is approximately 1/15 of the Carnot efficiency.

References

[1] D.M. Rowe, Thermoelectrics, an environmentally-friendly source of electrical power, Renew. Energy 16 (1999) 1251–1256.

[2] S. Kim, S. Park, S. Kim, S.H. Rhi, A thermoelectric generator using engine coolant for light-duty internal combustion engine-powered vehicles, J. Electron. Mater. 40 (2011) 812–816.

[3] M.A. Karri, E.F. Thacher, B.T. Helenbrook, Exhaust energy conversion by thermoelectric generator: two case studies, Energy Convers. Manag. 52 (2011) 1596–1611.

[4] J. LaGrandeur, D. Crane, S. Hung, B. Mazar, A. Eder, Automotive waste heat conversion to electric power using skutterudite, TAGS, PbTe and BiTe, in: International Conference on Thermoelectrics, 2006, pp. 343–348.

[5] Q.E. Hussain, D.R. Brigham, C.W. Maranville, Thermoelectric exhaust heat recovery for hybrid vehicles, SAE Int. J. Engines 2 (2009) 1132–1142.

[6] M. Mori, T. Yamagami, M. Sorazawa, T. Miyabe, S. Takahashi, T. Haraguchi, Simulation of fuel economy effectiveness of exhaust heat recovery system using thermoelectric generator in a series hybrid, SAE Int. J. Mater. Manuf. 4 (2011) 1268–1276.

[7] N. Baatar, S. Kim, A thermoelectric generator replacing radiator for internal combustion engine vehicles, TELKOMNIKA 9 (2011) 523–530.

[8] S.K. Kim, B.C. Won, S.H. Rhi, S.H. Kim, J.H. Yoo, J.C. Jang, Thermoelectric power generation system for future hybrid vehicles using hot exhaust gas, J. Electron. Mater. 40 (2011) 778–783.

[9] L.M. Goncalves, J. Martins, J. Antunes, R. Rocha, F.P. Brito, Heat-pipe assisted thermoelectric generators for exhaust gas applications, in: ASME 2010 International Mechanical Engineering Congress & Exposition, 2010, pp. 1387–1396.

[10] F.P. Brito, L.M. Goncalves, J. Martins, N. Antunes, D. Sousa, Influence of heat pipe operating temperature on exhaust heat thermoelectric generation, SAE Int. J. Passeng. Cars Mech. Syst. 6 (2013).

[11] J. Martins, L.M. Goncalves, J. Antunes, F.P. Brito, Thermoelectric exhaust energy recovery with temperature control through heat pipes, SAE Int. (2011).

[12] F. Yang, X. Yuan, G. Lin, Waste heat recovery using heat pipe heat exchanger for heating automobile using exhaust gas, Appl. Therm. Eng. 23 (2003) 367–372.

[13] R. Stobart, D. Milner, The potential for thermo-electric regeneration of energy in vehicles, SAE Int. (2009).

[14] A. Date, A. Date, C. Dixon, A. Akbarzadeh, Progress of thermoelectric power generation systems: prospect for small to medium scale power generation, Renew. Sustain. Energy Rev. 33 (2014) 371–381.

[15] P.D. Dunn, D.A. Reay, Heat Pipes, Pergamon, Exeter, Great Britain, 1994.

[16] H. Goldsmid, Bismuth Telluride and its alloys as materials for thermoelectric generation, Materials 7 (4) (2014) 2577–2592.

[17] N. Espinosa, M. Lazard, L. Aixala, H. Scherrer, Modeling a thermoelectric generator applied to diesel automotive heat recovery, J. Electron. Mater. 39 (2010) 1446–1455.